NUCLEAR INSTRUMENTS AND METHODS 156 (1978) 287-292 ; © NORTH-HOLLAND PUBLISHING CO.

# THE HELIX TUBE CHAMBER

OLAF ACHTERBERG, A. F. GARFINKEL*

*II. Institut für Experimentalphysik der Universität Hamburg, Hamburg, W. Germany*

G. FLÜGGE, H. JENSING, W. ZIMMERMANN

*Deutsches Elektronensynchrotron DESY, Hamburg, W. Germany*

H. MEYER and M. RÖSSLER

*Gesamthochschule Wuppertal, Wuppertal, W. Germany*

We report on the performance of a 1 m long position sensitive proportional tube. The position coordinate in the direction of the proportional wire is obtained to an accuracy of $\sigma = 3.9$ mm by means of a helical delay line. This proportional tube was designed for a large cylindrical detector system.

## 1. Introduction

The helix tube is a proportional tube providing good spatial resolution in the direction of the proportional wire ($z$-direction). The position of an ionizing particle passing through this detector is determined by measuring the time difference between the detection of the fast proportional wire signal and the cathode signal, which has to travel along a helical delay line. Similar delay lines have been built for the readout of multiwire proportional chambers[1]).

Important features of the helix tube are:

- The tubes are easily combined into large area helix tube chambers.
- There is negligible crosstalk of signals, since neighbouring tubes are decoupled by grounded outer shields.
- The complete collection of the charge gives rise to large cathode signals.
- The tubes are electrically and mechanically separated from each other, thus breaking of any high voltage wire affects only one tube, the loss of efficiency is small.
- The construction is of great mechanical stability.

We use a cylindrical system of 880 helix tubes to determine shower positions in a 1.2 m diameter barrel shaped lead-scintillator shower counter for the detector PLUTO[2]). PLUTO is a solenoidal magnetic detector for $e^+e^-$ colliding beam experiments at DORIS and PETRA. The magnetic volume contains 12 cylindrical multiwire proportional chambers enclosed by the barrel shower counter. Fig. 1 shows a section of the shower counter, which covers a solid angle of $0.53 \times 4\pi$ around the $e^+e^-$ interaction point. It consists of two rings segmented into 30 lead-scintillator sandwich modules each. The inner ring has a thickness of 3.9 radiation lengths, the outer ring of 4.7 radiation lengths.

In the gap between the two rings, two displaced layers of helix tubes localize the $z$ and $\phi$ coordinates of electromagnetic showers and of high energy particles. The helix tubes are combined to 10 modules with 88 tubes each.

## 2. Operation principle and tube construction

The operation principle of the helix tube is illustrated in fig. 2. Positive high voltage is applied to the proportional wire. A charged particle passing through the detector gives rise to a fast negative signal on the proportional wire. On the cathode an inverted signal is obtained. The cathode of the tube is built as a helical delay line with its axis parallel to the proportional wire. The conductors of the delay line are a wire helix and a grounded aluminium foil. The dielectric medium between the conductors, which is responsible for the specific delay line parameters, consists of glassfibre-epoxy material forming the wall of the proportional tube.

The signal propagating on the delay line reaches the electronics after a time proportional to the distance between the particle trajectory and the readout end of the tube. Hence, the position of an ionizing particle can be determined by measuring

* On leave from Purdue University, Lafayette, In. 47907, U.S.A.

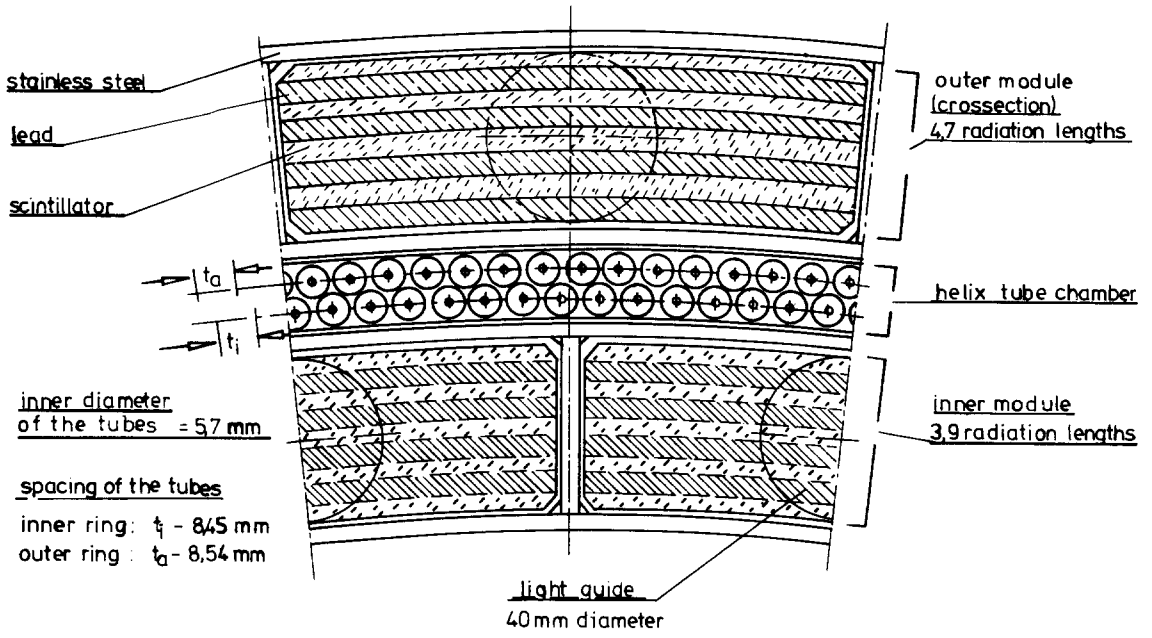


Fig. 1. A section of the barrel-shaped shower counter for the magnetic detector PLUTO. Two layers of helix tubes are situated between two lead-scintillator shower counter rings.

this propagation time. To compensate reflections, the ends of the helix are terminated with the impedance $Z_0$ of the delay line. The signals from the proportional wire and the helix provide the start and stop signals for a comparator digitizer. The data are recorded on a PDP computer. A block diagram of the digitizing electronics is shown in fig. 3. The resolution of the 11-bit time-to-digital converter is 0.5 ns. Since the cathode of the helix tube is built as an integrated delay line, there are no coupling losses and the cathode signal is comparable to the anode signal.

The delay line parameters can be calculated with the following equations. The capacity per unit length of the helix is given to good approximation by

$$C' = \frac{0.1772\varepsilon_r'}{(2a/h) + \ln(h/d)}\ (\mathrm{pF/cm})\ (\text{ref. 3}),$$

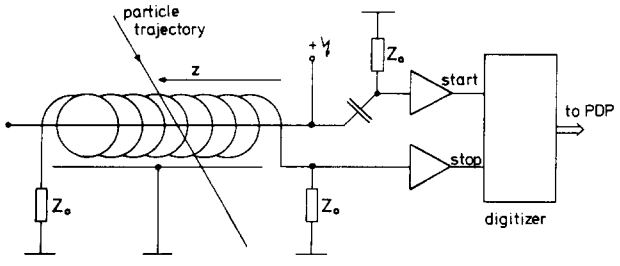


Fig. 2. Schematic view of the helix tube and principle of operation.

where (see fig. 4a)

$a$ = distance between helix and shielding (cm),
$h$ = Pitch of the helix (cm),
$d$ = Diameter of the helix wire (cm),
$\varepsilon_r'$ = relative dielectric number of the tube material, corrected for inhomogeneities.

With $d \simeq \frac{1}{2} h$ the simple equation

$$C' = 0.0886\ \varepsilon_r\ h/a\ (\mathrm{pF/cm})$$

can be used, where $\varepsilon_r$ = relative dielectric number of the tube material. The inductance per unit length is approximately given by

$$L' = \pi D/h\ (\mathrm{nH/cm})\ (\text{ref. 4}),$$

with $D$ = diameter of the helix (cm).

Neglecting the resistance of the helix wire, the impedance and delay time per unit length are (low frequency approximation)

$$Z_0 = \sqrt{(L'/C')}\ (\Omega),$$

$$t_0' = \sqrt{(L'C')}\ (\mathrm{s/cm}).$$

The length of the delay line is

$$s = (D+a)\ \pi\ l/h\ (\mathrm{cm}),$$

with $l$ = length of the proportional tube (cm). For the total delay of the helix we get in the low frequency approximation

$$t_0 = t_0' s\ (\mathrm{ns}).$$

and thus

$$t_0 \sim D^{\frac{3}{2}}.$$

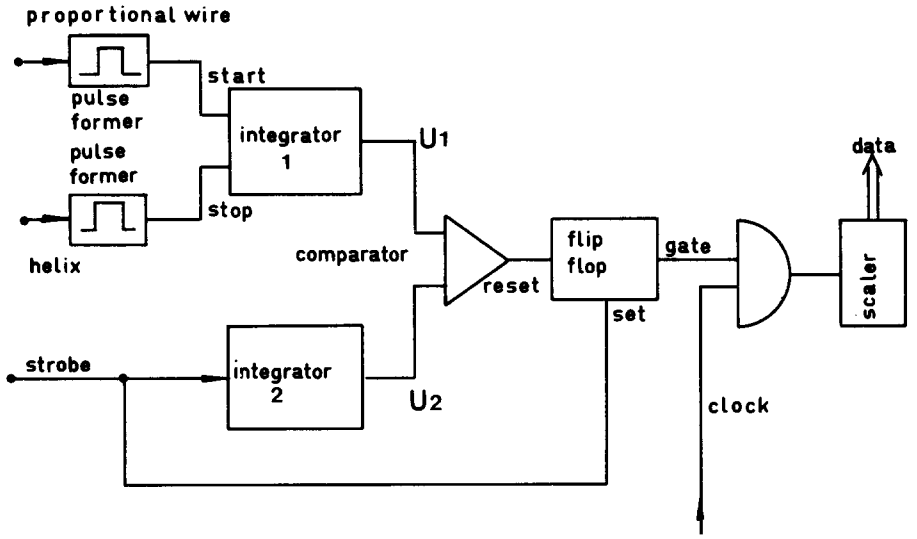


Fig. 3. Block diagram of the digitizing electronics.

We see that $t_0$ is very sensitive to variations in $D$. For typical proportional chamber signals the low frequency approximation is not sufficiently accurate. The total delay for cathode signals including high frequencies $f$ is given by

$t = t_0 \{1 - \frac{1}{2} (f/f_g)^2\}$ (ref. 5),

Where $f_g$ is the 3 dB cut-off frequency

$$f_g = \frac{\sqrt{3}}{\pi} \frac{Z_0}{R t_0},$$

and $R$ the resistance ($\Omega$) of the delay line. With $f \simeq f_g$ the total delay time is given by

$t \simeq 0.8\, t_0$

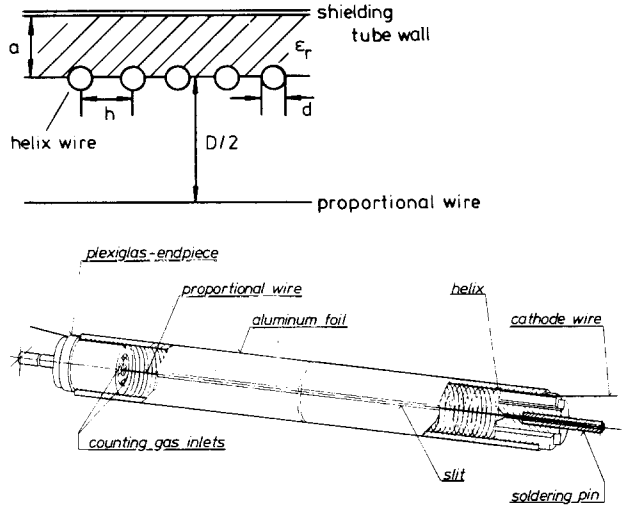


Fig. 4. (a) Definition of tube parameters. (b) Diagram of a helix tube.

Table 1 shows the dimensions of the helix tube and the measured and calculated values for the electrical parameters. We note good agreement between calculation and measurement for the impedance and delay time of the helix.

Fig. 4b shows a diagram of the helix tube. The construction of the tube involves a simple and inexpensive procedure. A helix of 200 $\mu$m Cu wire is wound with constant pitch on a metal rod coated with a teflon tube. A woven fibreglass tube is pulled over the helix and moistened with epoxy adhesive. After hardening of the adhesive, first

TABLE 1

Test chamber parameters.

| | | |
|---|---|---|
| a) *Geometrical parameters:* | | |
| distance helix to shielding | $a = 0.65$ mm | |
| pitch of the helix | $h = 0.5$ mm | |
| diameter of the helix wire | $d = 0.2$ mm | |
| diameter of the helix | $D = 5.9$ mm | |
| length of the test chamber | $l = 984$ mm | |
| b) *Electrical parameters:* | | |
| measured: | $\varepsilon_r = 5.05 \pm 0.05$ | |
| | $R = 22\,\Omega \pm 1\,\Omega$ | |
| calculated | $L' = 37.1$ nH/cm | |
| Capacity per unit length of the tube $C'$ | calculated 0.344 pF/cm | measured $(0.356 \pm 0.03)$pF/cm |
| Impedance $Z_0$ | 328 $\Omega$ | $(354 \pm 12)\Omega$ |
| Total delay $t$ | 366 ns | $(343 \pm 12)$ ns |

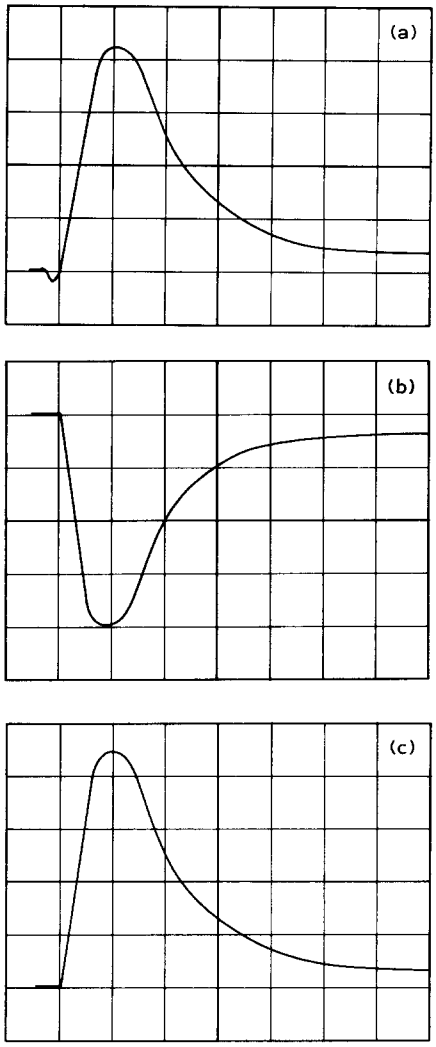


Fig. 5. Shape of the signals on anode and cathode of the helix tube as taken with a $^{60}Co$ source at an anode voltage of 1380 V. (a) Delay line signal, source near the readout end; vertical scale 20 mV/div., horizontal scale 100 ns/div. (b) Delay-line signal, source far from the readout end; vertical scale 20 mV/div., horizontal scale 100 ns/div. (c) Proportional wire signal; vertical scale 50 mV/div., horizontal scale 100 ns/div.

the metal rod and then the teflon tube can be removed.

For the proportional wire we use 30 $\mu$m gold-plated tungsten wire, stretched to a tension of 50 g. The wire is fastened on plexiglass endpieces which also provide the gas inlets. An aluminium foil is glued on the outside of the tube and serves as ground potential for the delay line. The grounded shielding has a small slit along the tube. A closed aluminium shielding would provide a current path around the circumference of the tube

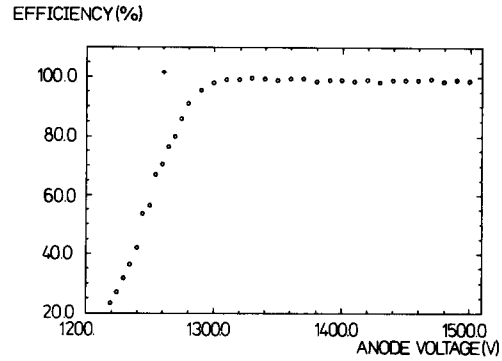


Fig. 6. Efficiency plateau curve of the test chamber.

and generate a contra-inductance which deteriorates the pulse shape.

## 3. Test results

For test purposes we constructed a chamber consisting of 8 helix tubes arranged in two layers. The distance between the proportional wires is 8.5 mm and the layers are displaced by 4.25 mm. As operating gas mixture we used 90% argon and 10% propane. After preamplification by a factor of 4 for the proportional wire signals and a factor of 8 for the delay line signals the threshold of the read-out electronics was set to 5 mV.

Typical signals from anode and cathode of a helix tube are shown in fig. 5. The shape of the delay line signals does not change substantially with the distance from the readout side of the helix tube. Cathode signals generated by particles crossing the detector near the readout end have a risetime of 45 ns*. Due to the dispersion of the signals on the electromagnetic transmission line, caused by the resistance of the helix wire, the rise-

* The risetime was measured with an input impedance of 600 $\Omega$ parallel to 140 pF.

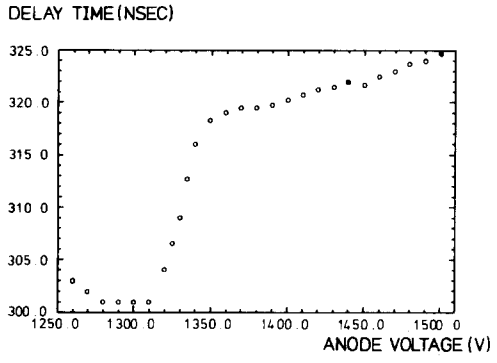


Fig. 7. Delay time vs anode voltage.

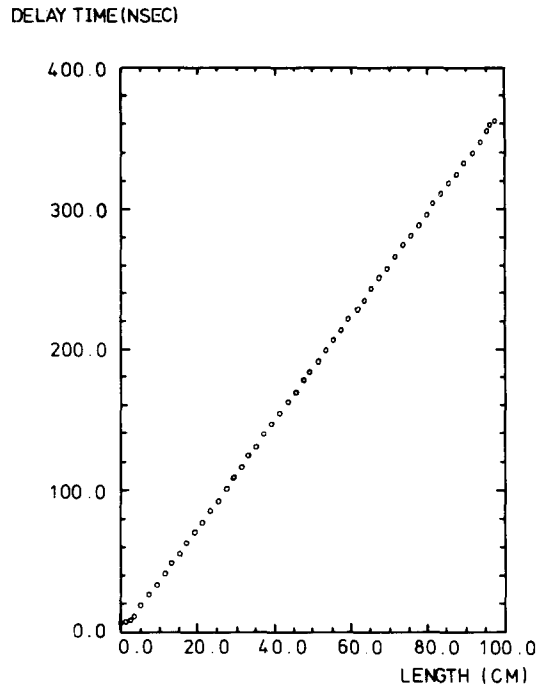


Fig. 8. Linearity of the helix tube.

time increases to 55 ns at the far end of the detector. The loss of amplitude is about 5%.

To determine the detection efficiency of the test chamber described above as well as the linearity and the position resolution of the individual tubes, we used a $^{106}$Ru $\beta$-source collimated to 1.5 mm diameter. The electron trajectories through the chamber were defined by a coincidence of two 3 mm diameter scintillation counters placed in front and behind the helix tube chamber.

With this experimental set-up we measured a detection efficiency of more than 99.5% relative to the scintillation counters, with no dependence on the position along the detector. Fig. 6 shows the plateau curve of the test chamber.

The crosstalk between the individual tubes in the test chamber was measured to be less than $2\times10^{-3}$.

At an anode voltage of 1410 V, the first Geiger pulses appeared in the test chamber. In tests with cosmic muons the detector operated without breakdown at anode voltages up to 1700 V.

To determine the optimal working range of the helix tube, we measured the delay time versus anode voltage with the $\beta$-source at constant position $z$. Fig. 7 shows the measured curve for $z=90$ cm. Near 1380 V both efficiency and delay time have reached a plateau and no Geiger pulses occur. The linearity of chamber and electronics was determined by moving the source in steps of 20 mm along the tubes. The position of the source was adjusted with an uncertainty of $\pm0.1$ mm. Fig. 8 shows the linearity curve. The measured points were fitted to a straight line. Neglecting the end

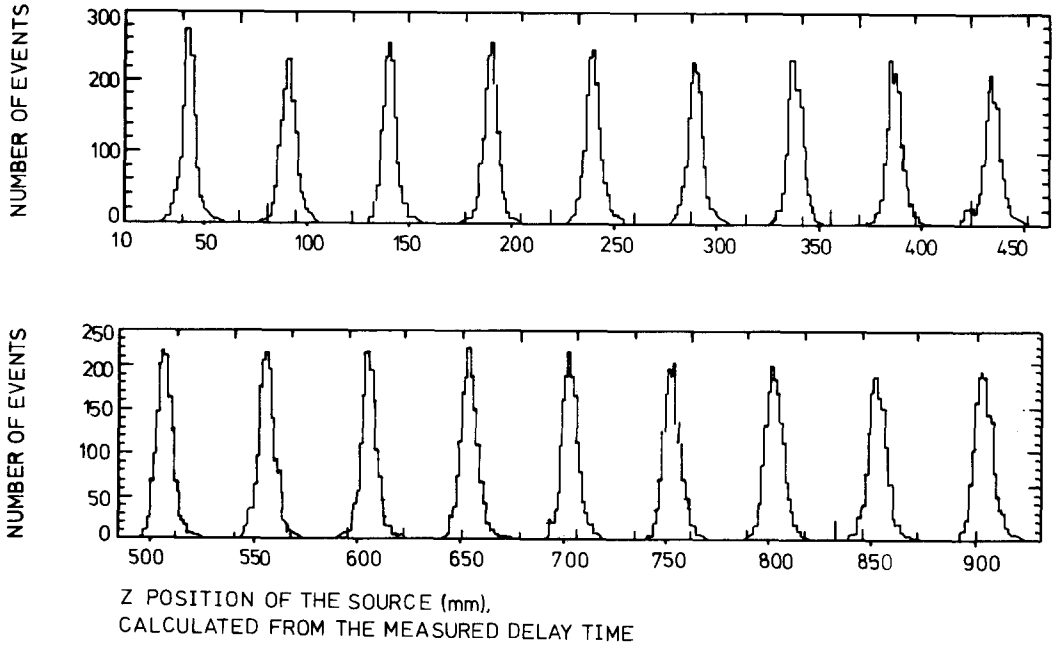


Fig. 9. Position resolution of the helix tube, measured with a $^{106}$Ru source. The source was moved in steps of 50 mm.

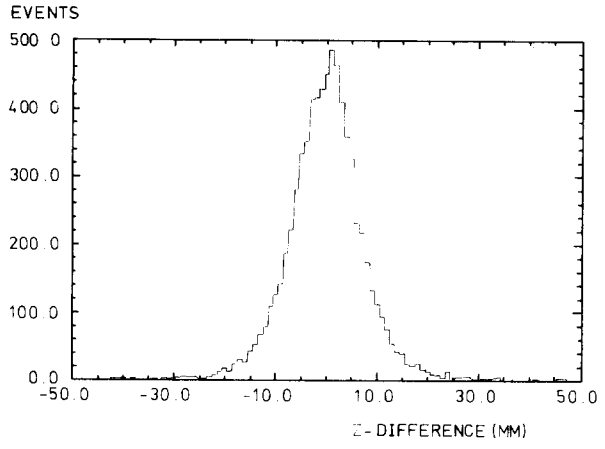


Fig. 10. Differences of the $z$-positions measured in two overlapping tubes, corrected for inclined tracks.

effects the mean deviation from the fitted curve is 0.75 ns for a typical helix tube. This corresponds to a nonlinearity of $\sigma_{\text{lin}} = 2.0$ mm averaged over the whole tube length.

Again using the $^{106}$Ru source, the position resolution in $z$ was measured. Fig. 9 shows the results of a scan over the whole tubelength, the source being moved in steps of 50 mm. From this measurement the position resolution $\sigma_p$ of the helix tube was determined to be better than 3.7 mm. Correcting for the divergence of the electrons from the radioactive source yields a resolution of $\sigma_{\text{corr}} = 3.6$ mm, which is compatible with the width of all observed peaks. Due to the dispersion of the signal mentioned above, the resolution depends on $z$ with a maximum variation of $\pm 15\%$ over the tube.

## 4. Properties of a detector with 880 tubes

A calibration of the array of 880 tubes described above was made in the detector PLUTO. Cosmic ray tracks detected in the proportional chambers of the inner detector were extrapolated through the helix tube chamber. The calculated intersection point was compared with the position measured in the tube chamber.

The $z$-resolution was obtained from tracks which intersected two overlapping tubes (see fig. 1). Fig. 10 shows the difference in the $z$-values from the two tubes corrected for inclined tracks and averaged over the whole detector. The resulting mean $z$-uncertainty is $\sigma = 3.9$ mm, due to the nonlinearity of the tubes and electronics and the inherent position resolution. This value is well accounted for by the position resolution and the linearity measured with the $^{106}$Ru source (see section 3).

In the direction transverse to the proportional wire, the position resolution of a single tube is equal to its inner diameter. The use of two or more displaced layers of helix tubes results in 100% detection efficiency as well as in an improved spatial resolution.

We are indebted to A. Marxen, H. Schultz and A. Stüben for the construction of the helix tubes and the cylindrical chamber.

We thank H. Ahrens, R. Cyriacks, K. Finke and H. Kock for their help in the construction and tests of the helix chambers. We acknowledge the help of W. Mehrgardt and R. Pforte during the set-up of the readout software.

## References

1) R. Grove, I. Ko, B. Leskovar and V. Perez-Mendez, Nucl. Instr. and Meth. **99** (1972) 381; D. M. Lee, J. E. Sobottka and H. A. Thiessen, Nucl. Instr. and Meth. **109** (1973) 421; A. Breskin, G. Charpak, F. Sauli and J. C. Santiard, Nucl. Instr. and Meth. **119** (1974) 1.

2) L. Criegee et al., Proc. 1973 Int. Conf. on *Instrumentation for HEP*, Frascati (1973); PLUTO-Collaboration, J. Burmester et al., Phys. Lett. **64B** (1976) 369.

3) W. Zimmermann, Die Wendelrohrkammer (1975) unpublished.

4) Meinke–Gundlach, *Taschenbuch der Hochfrequenztechnik* (Springer Verlag, Berlin, 1956).

5) H. E. Kallmann, Proc. IRE **34** (1946); J. Blewett and J. H. Rubel, Proc. IRE **35** (1947).